



Microfabricated planar glass gas chromatography with photoionization detection

Alastair C. Lewis^{a,*}, Jacqueline F. Hamilton^b, Christopher N. Rhodes^b, Jaydene Halliday^b, Keith D. Bartle^c, Philip Homewood^d, Robin J.P. Grenfell^e, Brian Goody^e, Alice M. Harling^e, Paul Brewer^e, Gergely Vargha^e, Martin J.T. Milton^e

^a National Centre for Atmospheric Science, University of York, Heslington, York, YO10 5DD, UK

^b Department of Chemistry, University of York, Heslington, York, YO10 5DD, UK

^c Energy and Resources Research Institute, University of Leeds, Woodhouse Lane, Leeds, LS2 9JT, UK

^d The Dolomite Centre, Unit 1, Anglian Business Park, Orchard Road, Royston Herts., SG8 5TW, UK

^e National Physical Laboratory, Hampton Road, Teddington, Middlesex, TW11 0LW, UK

ARTICLE INFO

Article history:

Received 5 October 2009

Received in revised form

26 November 2009

Accepted 2 December 2009

Available online 4 December 2009

Keywords:

Gas chromatography

Microfabrication

Volatile organic compounds

Photoionization

Field instrumentation

ABSTRACT

We report the development of a microfabricated gas chromatography system suitable for the separation of volatile organic compounds (VOCs) and compatible with use as a portable measurement device. Hydrofluoric acid etching of 95 × 95 mm Schott B270 wafers has been used to give symmetrical hemispherical channels within a glass substrate. Two matching glass plates were subsequently cold bonded with the channels aligned; the flatness of the glass surfaces resulted in strong bonding through van der Waals forces. The device comprised gas fluidic interconnections, injection zone and 7.5 and 1.4 m long, 320 μm internal diameter capillaries. Optical microscopy confirmed the capillaries to have fully circular channel profiles. Direct column heating and cooling could be achieved using a combination of resistive heaters and Peltier devices. The low thermal conductivity of glass allowed for multiple uniform temperature zones to be achieved within a single glass chip. Temperature control over the range 10–200 °C was achieved with peak power demand of approximately 25 W. The 7.5 m capillary column was static coated with a 2 μm film of non-polar dimethylpolysiloxane stationary phase. A standard FID and a modified lightweight 100 mW photoionization detector (PID) were coupled to the column and performance tested with gas mixtures of monoaromatic and monoterpene species at the parts per million concentration level. The low power GC-PID device showed good performance for a small set of VOCs and sub ng detection sensitivity to monoaromatics.

© 2009 Elsevier B.V. All rights reserved.

1. Introduction

During the last 50 years gas chromatography has developed into one of the most widely used of the chemical analysis techniques. It is a simple, rapid and highly sensitive tool that provides efficient separation of components in mixtures and has an almost complete spectrum of applications. In combination with a flame ionization detector (FID) or a mass spectrometer (MS), it forms one of the most powerful tools for environmental gas analysis, and has been used in many studies to measure volatile organic compounds (VOCs) [1–4]. Despite a high degree of current commercial instrument sophistication, modern GC systems remain bulky and fragile, as well as being power intensive – typically up to 3 kW peak. The heating of GC columns has evolved relatively little over the past 40 years, based generally on the turbulent fan oven, which remains the most efficient means of evenly heating the intricate structure of a wound

capillary on a spindle or bobbin. The nature of GC and the size of such an oven make it a difficult technique to use in remote or hostile locations for environmental research.

There is great potential in this area therefore for microfabricated GC systems that are compact, robust and with low power demands, and a short review of relevant literature follows this section. There is particular intrinsic attraction in monolithic GC structures, where all components of the device (injector, column, detector) are formed in a single fabrication step with benefits for robustness, lack of interconnections, and a structural geometry that is very much easier to heat using planar devices. This paper reports the development of a microfabricated and miniaturized glass gas chromatographic system as a potential means to overcome some of the portability limitations associated with drawn capillary columns and turbulent fan GC ovens.

Miniaturized and microfabricated GC systems are not a new proposition; the first gas chromatograph fabricated in silicon using photolithography and chemical etching techniques was reported in 1975 by Terry et al. at Stanford University [5]. The micro-GC consisted of an injection valve and a 1.5 m long column with a depth of

* Corresponding author.

E-mail address: acl5@york.ac.uk (A.C. Lewis).

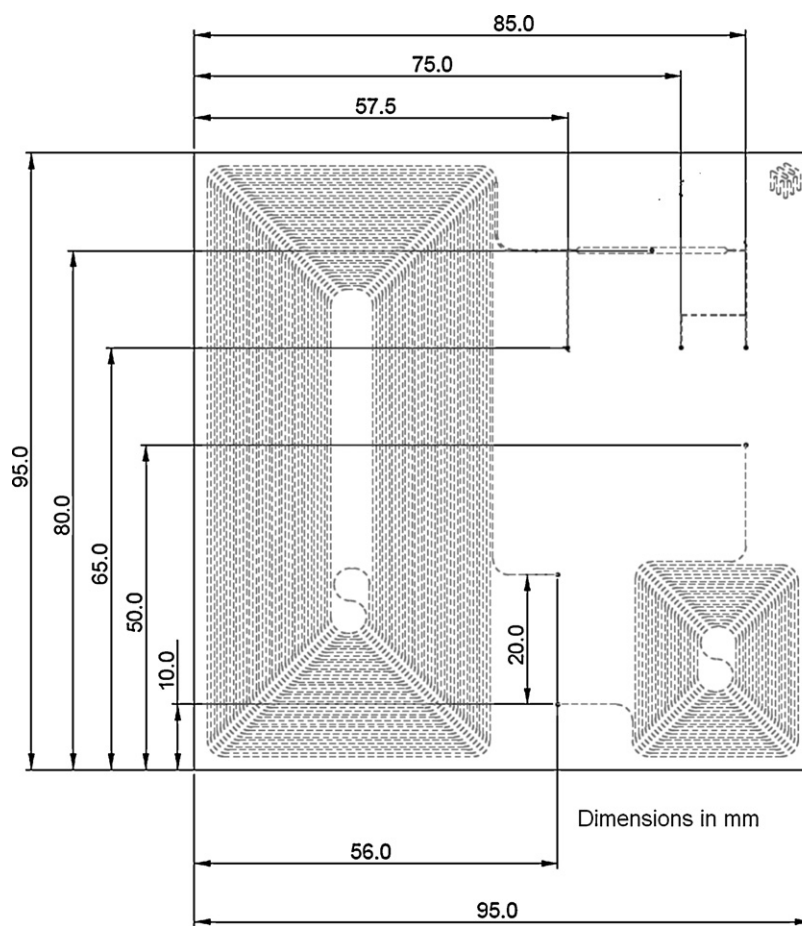


Fig. 1. Basic layout of the GC device including main GC column of 7.5 m length, injection zone and 1.4 m length second column (not used in this study).

40 μm and a width of 200 μm fabricated on a silicon wafer, with an internally mounted thermal conductivity detector (TCD). The spiral column had a rectangular cross-section, and the silicon wafer was hermetically sealed to a Pyrex glass cover plate [5]. The resolving power of the column was poor in comparison to standard columns of the day. A number of factors contributed to this, not least the difficulty in evenly coating rectangular channels and that the majority of the other GC components were not miniaturized. Since that time there has been a great deal of research undertaken to develop silicon fabricated on-chip electrophoresis and liquid chromatography systems, but with chip-based gas chromatography receiving somewhat less attention. Recent examples of microfabricated GC systems for VOC measurement include those reported by Sandia laboratories [6,7] incorporating a preconcentrator consisting of a thin silicon nitride membrane supporting a patterned metal film-heating element, a 1 m long $100 \times 400 \mu\text{m}$ high aspect ratio GC column on a silicon wafer, and an array of surface acoustic wave (SAW) sensors.

Silicon has been very much the favoured substrate to date for microfabricated GC columns generally using the Dry Reactive Ion Etching (DRIE) method, followed by a Pyrex cover sheet being anodically bonded to the wafer yielding a sealed GC column. Many silicon examples can be found in the literature [8–15] with non-polar dimethylpolysiloxane and moderately polar trifluoropropylmethyl polysiloxane phases giving columns with between 3500 and 8200 plates [16–18].

Although silicon dominates the literature as a substrate, columns have been made in other materials including porous silicon [19], carbon nanotubes [20], parylene [21], metal [22,24] and ceramic [23]. In addition, a variety of fabrication techniques have

been utilised including DRIE, DRIE polymer vapour deposition, stereolithography, silicon bulk micromachining, and Lithographie, Galvanoformung, Abformung (LiGA).

Of the miniaturized devices previously reported, a common feature has been the use of square sided channels to form the separating column. The greatest difficulty associated with column coating is therefore in achieving a uniformly thin layer of the desired thickness right across the cross-section of the column including the corners. A limitation of rectangular designs is “pooling” of the stationary phase at the column corners producing an uneven thickness of stationary phase. Peak broadening and general degradation of the separation performance may result from analytes spending a longer time in these areas of thicker coating [25]. Limited numbers of circular channelled microfabricated devices have been reported, notably by Potkay et al. who reported columns of 1 m length and 90 μm diameter with a semi-circular cross-section [8] and Pai et al. reporting the use of circular cross-sectional silicon serpentine columns with a 250 μm internal diameter [26].

Various detectors have been reported in conjunction with micro-GC systems. TCD is one of the few miniaturized detectors commercially available and has been reported in the literature a number of times [5,27–29]. Other detectors, such as surface acoustic wave (SAW) devices [6,7,30], differential mobility spectrometers [11], FID [23], metal oxide gas sensors [12,13] and nanoparticle-coated chemiresistors [18] and carbon nanotubes based ionization detectors [31], offer promise of miniaturization and integration with columns. Micro-FID has shown results comparable to conventional flame photometric and flame ionization detectors, thus making it also a potentially useful detector when used in combination with a micro-GC system [32–34].

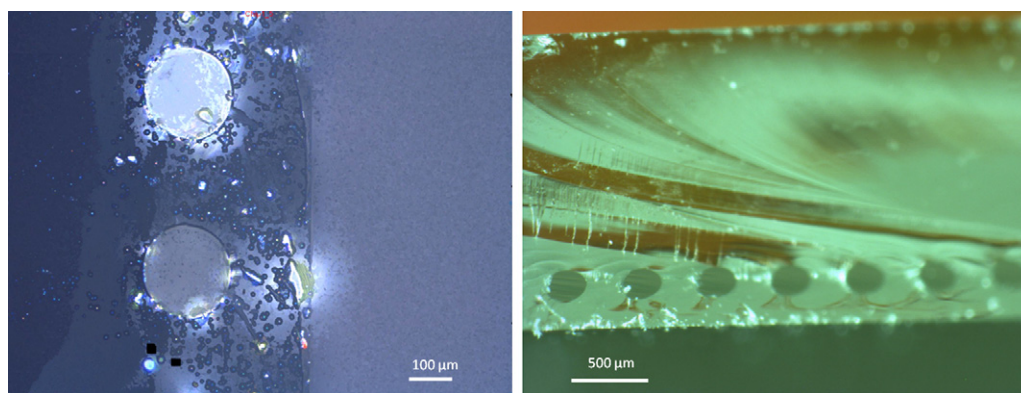


Fig. 2. (a) Shows a cross-section of the glass device taken using a Alicona G4 Infinite Focus microscope, (b) the same glass section using a Wild Heerbrugg M400 microscope. Measurements of three bores in (a) give internal column diameters of 242, 250 and 248 μm with a manufacture target of 250 μm . (b) Shows how the use of an asymmetric pair of glass thicknesses places the GC channels within a few hundred microns of one surface of the device for direct heating.

We report here the development of a planar microfabricated GC system that uses acid etched borosilicate glass as the working substrate. This approach results in capillary channels that are circular in cross-section and similar in dimensions to drawn capillary columns. The cost and ease of glass fabrication in this manner is attractive when compared to silicon, allowing a column of 7.5 m length and 320 μm i.d. to be fabricated in a 40 \times 85 mm section of glass, part of a larger 95 \times 95 mm monolith containing also a injection unit and additional columns for multidimensional GC. For non-polar species glass offers a useful material of column manufacture and with performance potentially equivalent to that of fused silica. Glass is a less appropriate material for polar organic analysis however, and hence we see the major application of this technology lying in the areas of hydrocarbon and VOC analysis.

The use of a miniaturized photoionization detector in conjunction with the glass column is also reported. The overall system had an attractive peak capacity and detection limit for VOCs, low power demand and an operating temperature range of 10–200 $^{\circ}\text{C}$ without cryogenics. This we believe offers an alternative material route to enable microfabricated GC systems.

2. Experimental

2.1. Glass fabrication

The glass device was fabricated by a specialised manufacturer of micro-scaled glass devices (Dolomite Centre, UK). The design used two glass (Schott B270) wafers (one 0.5 mm thick, the second 2.5 mm thick) with etched channels bonded together to form

a single “chip”. The general layout of the columns and dimensions is shown in Fig. 1. The etching was carried out chemically. The surface of each half of the glass chip was covered with a chrome layer then a photoresist layer. These layers were sequentially etched leaving a patterned layer on the surface of the chip that defines the glass channels during the etching of the chip. The first step was to expose the photoresist layer to UV light through a mask outlining the channels. The photoresist exposed to the UV light becomes soluble to the photoresist developer whereas the unexposed photoresist remains insoluble. The developer removes the exposed photoresist leaving an engraved pattern of the channels. These channels are then used to etch the chrome layer. Finally the glass is wet etched with hydrofluoric acid solution along these preformed channels. The HF etching process is controlled to ensure symmetrical, hemi-spherical channels. After the photoresist and chrome layers are fully removed the halves of the chip are then cold bonded; the two halves are brought into contact, with the channels aligned, and the flatness of the glass surfaces results in strong bonding through van der Waals forces. No heating is required for bonding and chips fabricated using this process can withstand pressures up to 50 bar.

Fig. 2a and b shows a cross-section of a portion of a glass chip obtained using a Alicona G4 Infinite Focus microscope and Wild Heerbrugg M400 microscope. Both figures clearly show the uniformity of the column, the accurate alignment of the two halves of glass and that the profile is very close to circular. Measurements of three bores from Fig. 2a (only two visible in figure) give internal column diameters of 242, 250 and 248 μm in a chip with a target internal diameter of 250 μm . [Note these photographs were taken

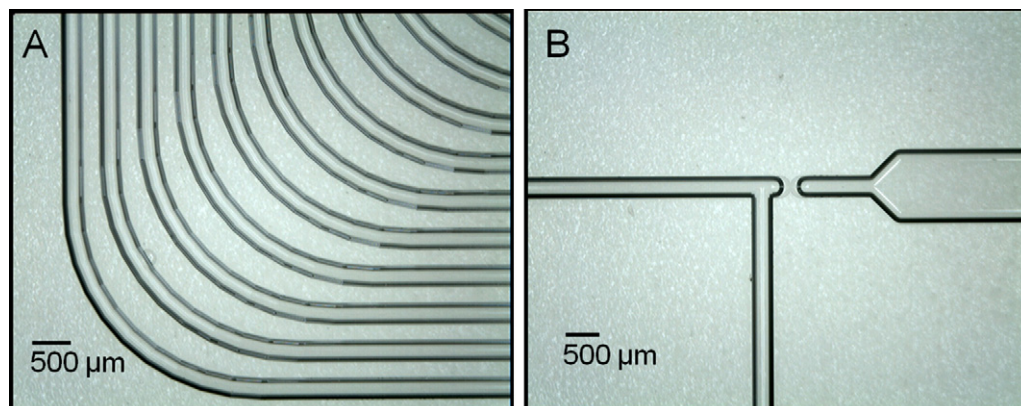


Fig. 3. Left: close up image of column turns; right close up image of injector (1 mm wide, 0.3 mm deep) region coupled to 7.5 m column via a 50 μm restrictor region.

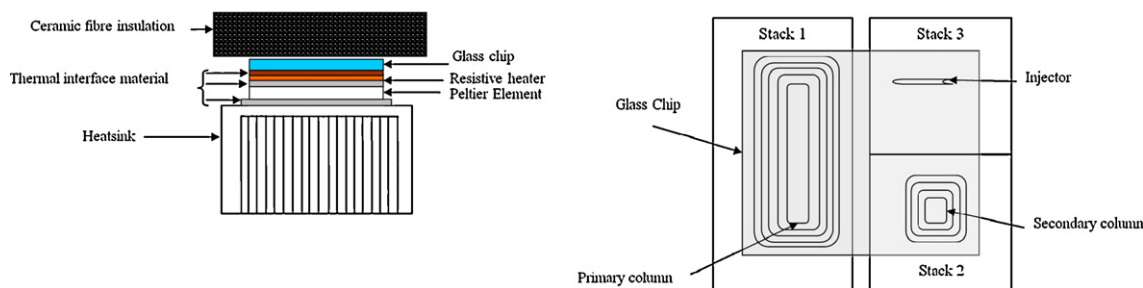


Fig. 4. (a) Side view showing the layout of components in the temperature controlled stack used for heating and cooling the glass GC. (b) Plan view layout of the temperature controlled stacks. Stack 1 is under the primary 7.5 m long column. Stacks 2 and 3 are positioned under the secondary 1.4 m column (not used here) and the injection region, respectively.

of a chip with different internal diameter to that used to generate the chromatograms in later figures]. Fig. 2b shows how the use of an asymmetric pair of glass thicknesses places the GC channels within a few hundred microns of one surface of the device for direct heating.

Fig. 3 shows a close up of the column spiral and also a close of the end section of an etched injection unit (1 mm wide and 0.32 mm deep) which is coupled to the column via a restricting pinch at the injector outlet.

2.2. Thermal profile and thermal control

Uniform heating of a GC column is central to its performance requiring accurate and reproducible column temperatures and with minimal spatial temperature gradients. For the device reported here, a combination of direct heating approaches have been investigated. These have included the direct heating of the glass wafer with metal heating elements placed above and below the device, and a more complex arrangement involving a stack of thin film resistive elements and Peltier devices. An example of the latter arrangement is shown in Fig. 4a in side view. Since glass is a relatively poor heat conductor, the separation of the zones of the device allows, in principle, the differential heating of the injector from the columns and other regions. We test this using three different control thermal stacks and temperature zones shown in Fig. 4b. The heater consisted of a polyimide encapsulated heater manufactured by Minco, Minneapolis, US. The Peltier devices were silicone sealed TEC 12715HTS units manufactured by Merit Technology, Shenzhen, China. The Peltier elements were bonded directly to

a finned aluminium heatsink using thermally conductive epoxy adhesive. The heatsink was equipped with a centrifugal blower for rapid cooling of the metal fins. The total mass of stack 1 beneath the primary column, including the blower was 250 g and an overall height of 6 cm.

Temperature monitoring of the stack was achieved using a PT100 polyimide encapsulated sensor placed between the heater and the glass chip. A configurable CompactRIO module supplied by National Instruments running Labview Realtime operating system was used to control the temperature of the stack. The CompactRIO embedded system regulated the power delivered to the heater and Peltier units by modulating the on-off duty cycle of a 10 kHz signal. In this way the power to the heaters and Peltier devices could be continuously varied between 0 and 100%. A proportional integral derivative algorithm was used to minimize temperature offset and oscillation during temperature programming. A polarity reversal switch in the Peltier power supply enabled the devices to operate in two modes: (1) heat extraction mode transferring heat from the GC chip to the heatsink and; (2) temperature enhancement mode transferring heat from the heatsink to the GC chip. In addition the heatsink blower would be switched on during heat extraction mode to improve dissipation of heat to the surrounding air.

In many situations thermal imaging devices can be used to determine the distribution of temperatures across the surface of an object. However, to do so in this case would require the removal of the top layer of ceramic fibre insulation used to prevent heat loss to the surroundings. Rather, we determine the temperature profile across the chip using a matrix of sixteen temperature sensors. Thick film platinum resistance temperature sensors (Labfacility DM503

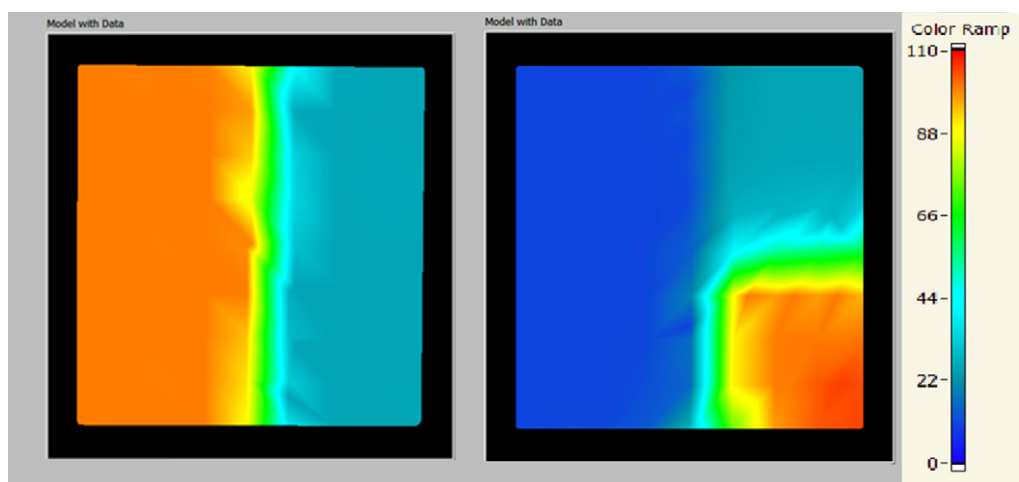


Fig. 5. (a) Measured temperature profile with stack 1 (under the 7.5 m column) heated to 100 °C, all other stacks left at ambient. (b) Measured temperature profile when stack 1 was cooled to 10 °C whilst holding the temperature of stack 2 (the 1.4 m column) at 100 °C. The temperature remained uniform (± 2 °C) over stack 1 and the unheated stack 3 remained at ambient temperature.

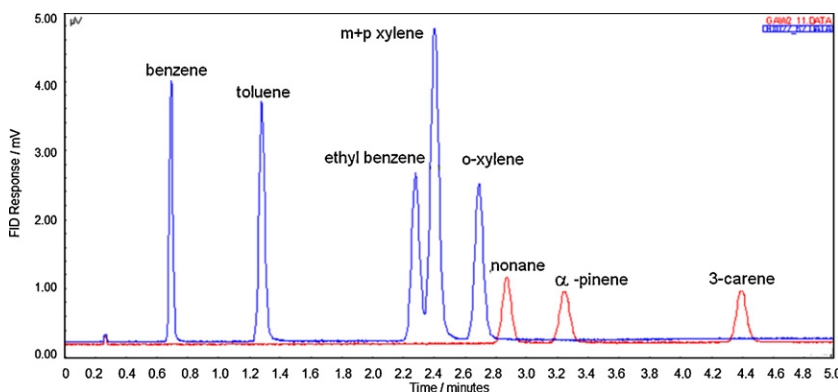


Fig. 6. Separation using a 7.5 m long, 320 μm internal diameter planar glass column with 2 μm OV101 stationary phase, placed in a GC fan oven and with commercial FID (Varian 3800). Blue trace is an injection of the BTEX standard mixture and red trace a mixture of 2 ppm nonane, alpha-pinene and 3-carene (red) with a 0.5 mL sample loop. (For interpretation of the references to colour in this figure legend, the reader is referred to the web version of the article.)

with resistance tolerance to Class A DIN IEC 751) were attached across the chip surface in an X pattern using thermally conductive epoxy adhesive. The sensors were connected to the interface by means of three core screened cable which was routed between the top side of the glass chip and the ceramic fibre insulation. The excitation current for each sensor was maintained at 1 ± 0.03 mA using a STMicroelectronics LM334Z constant current source. The resulting voltage developed across each resistance sensor was digitized using a National Instruments USB 6210 analog to digital convertor. The data collected was converted to temperature using the Callendar Van-Dusen equation with polynomial coefficients of $A = 3.9083 \times 10^{-3}$ and $B = -5.775 \times 10^{-7}$. The temperature data were displayed in the form of a colour map overlaid on a two dimensional image of the glass chip using Labview software from National Instruments.

Fig. 5a shows the temperature profile across the surface of the chip when stack 1 (7.5 m column) is heated to 100 °C. Stack 2 and stack 3 beneath the 1.4 m column and preconcentrator were not heated. It is interesting to note that there is very little heat transfer between the heated side of the chip and the unheated side, which remained at an ambient temperature of 22 °C. This is due partly to the low thermal conductivity of glass and the 1 cm air gap between stack 1 and stacks 2 and 3. Temperature uniformity across the area of the chip over stack 1, i.e. the 7.5 m column, was within ± 2 °C of the setpoint. Fig. 5b shows the temperature profile across the chip surface when stack 1 is cooled to 10 °C using the Peltier devices and with stack 2 heated to 100 °C. The 2D images reveal that the divided thermal stack arrangement is capable of independently controlling the temperature of at least three discrete regions of the glass GC device. The temperature gradient across the glass chip during temperature ramping was determined by comparing data from two temperature sensors located on the heated and non-heated side of the chip. During temperature ramps of 5°, 10° and 20° per minute the temperature difference between the bottom and lower surfaces was 3°, 8° and 15°, respectively. Since the column is contained within a 0.320 mm depth of the chip the calculated temperature gradient across the column is 0.3°, 0.7° and 1.3° at ramp rates of 5°, 10° and 20° per minute. Using this arrangement a minimum column temperature of 3 °C was achieved at an ambient air temperature of 22 °C and a maximum of 200 °C with linear ramp rates of between 5 and 20 °C/min. Typical power consumption was 25 W mean or 30 kJ per analysis.

2.3. Column coating

A “static” procedure was used to deposit a film of a non-polar dimethylpolysiloxane stationary phase (OV-101, Restek) on the

inside of the column. The column was filled with a solution containing the stationary phase prior to controlled evaporation of the solvent. This method is used widely to deposit a highly uniform film, which can be difficult to produce by a dynamic method based on pumping solution through the column. Pentane was used to dissolve the stationary phase into a solution at 3.8% (by volume). The column was placed inside a vacuum oven (Thermo Scientific) at room temperature and left for several days, with the pressure maintained between 10 and 40 kPa below atmospheric.

The column was weighed periodically with a laboratory balance with an uncertainty of ± 0.2 mg (95% confidence) to monitor the evaporation of the solvent. Open vials of pentane were placed inside the vacuum oven. The saturated vapour of the pentane restricted the vacuum at the start of the process, and thus acted as a pressure buffer. The vacuum was maintained at a level that was too low to initiate boiling of the solvent within the column as indicated by the absence of boiling in the pentane vials. After 2 days of slow evaporation at ambient temperature the temperature was increased to 50 °C and the pressure decreased to 100 kPa below atmospheric. After 4 days all of the pentane was removed and the chip was re-weighed to confirm the mass of stationary phase deposited. Calculation shows that the mass of 11 mg of stationary phase deposited was equivalent to a uniform layer 2 μm thick.

Capillary transfer and split lines were bonded into the column ports using Shellac, a resin suitable for bonding the capillary onto glass. The resin is easily moulded upon heating and forms a gas tight seal when it cools, after which it remains intact at temperatures in excess of 200 °C.

2.4. Separation performance in a laboratory GC with FID

The coated chip was tested using the fan oven, temperature control, injection and flow control systems of a laboratory gas chromatograph (Varian 3800). This enabled the separation capabilities of the coated glass column to be characterised with an established FID. High purity helium (BIP Air Products, Keumiee, Belgium) was used as the carrier. The chip was connected to the GC system via a capillary, which was held in place using a resin (shellac). The capillary was connected to the detector of the GC as it would usually be, using the GC’s internal connectors.

A standard BTEX mixture including 10 $\mu\text{mol/mol}$ (molar ppm) of benzene, toluene, *m*-xylene, *p*-xylene and *o*-xylene was injected via a 0.5 cm^3 gas sample loop. A second ppm gas mixture of nonane, α -pinene and 3-carene was injected separately. The BTEX/terpene mixtures were flowed at $\sim 20 \text{ cm}^3 \text{ min}^{-1}$; the electronic flow control for the column was set at $12 \text{ cm}^3 \text{ min}^{-1}$. Automated valve changes, as part of the Varian 3800 GC system, were used. The oven

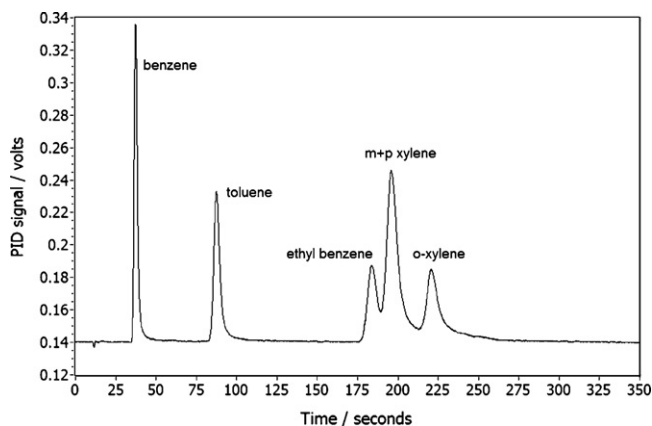


Fig. 7. Separation of the 10 ppm BTEX standard gas mixture. 0.5 mL sample loop in combination with the planar glass 7.5 m GC column programmed from 10 to 100 °C at 20 °C/min heated using Peltier and resistive elements. Detection is by low power photoionization detector.

was programmed to run at 30 °C for 0.2 min, then ramp at 20 °C/min to 100 °C. The switching valve was heated to 170 °C.

The results are shown in Fig. 6, which shows good separation between all of the injected components with symmetrical peak shape and with elution in 4 min. Peak skew is less than 1.8 for all peaks (the majority less than 1.3) which we considered acceptable. The chromatogram indicates around 2000 theoretical plates as measured for toluene.

2.5. Performance with direct resistive heating and PID

Following characterisation of performance in a standard lab GC the glass column was tested with direct heating (similar to that described in early sections) using manual loop injections. A low cost and low power photoionization detector (PID) operating with a lamp with an ionization potential of 10.6 eV was attached to the column outlet (Alphasense, Great Notley, manufacturers part code PID-AH, 100 mW nominal power consumption at 3.0 V and 8 g mass).

A two-stage regulator was used to provide constant head pressure of helium carrier and was connected to a 6-port valve (VICI, TX, USA) and operated manually. A 0.2 cm³ sample loop made from treated stainless steel was fitted to the valve in a configuration to allow sample filling in one position and sample injection in the other. During sample filling the standard gas mixture flowed through the valve and the sample loop for a minimum of 5 min. During injection, the carrier gas flowed through the sample loop for a short time to direct the sample onto the chromatographic column. The duration of the injection was selected to ensure all gas in the loop was flushed onto the column but was limited to prevent peak tailing from compound desorption from the metal surfaces. The 6-port valve was connected to the inlet of the chip by a 1/16" Silcosteel tube (length 10 cm) and a 0.32 mm inner diameter fused silica capillary (20 cm length) connected by a reducing union (Thames Restek, Saunderton, UK).

The eluent from the 7.5 m long column was connected to the PID by 0.32 mm inner diameter uncoated fused silica capillary. The detector was integrated into the unit and to a data acquisition system. The carrier gas head pressure was set to 300 Pa providing a column flow of 12 cm³ min⁻¹. The value deviates from theoretical calculations due to the presence of 50 μm pinch point regions before and after the etched injector (see Fig. 3). We introduced a 1:5 split at the column outlet in order to prevent detector saturation, and hence the flow rate arriving at the PID was measured to be 1.8 cm³ min⁻¹.

The BTEX standard gas mixture was injected onto the column at starting temperature of 10 °C using the manual gas sampling valve. A temperature ramp of 20 °C/min up to 100 °C was applied. As seen in Fig. 7, chromatographic separation was sufficient to resolve *o*-xylene in around 225 s. The high PID response of aromatic compounds ensured a good signal to noise ratio. The chromatogram generated shows good peak shapes and height from the injection of approximately 1.5 ng of each compound. Detection limit with the PID was estimated to be of the order 100 pg for benzene.

3. Conclusions

A fully circular profile gas chromatography column has been microfabricated from glass using acid etching techniques. The use of glass has allowed for relatively long column lengths and standard internal diameters to be achieved in addition to the inclusion of other components on to a glass wafer. Direct resistive heating and cooling of the glass chip produced a uniform heating profile across the 7.5 m column when held at both above and below ambient temperatures. The low thermal conductivity of glass allowed for multiple temperature zones within the same chip. The power required to achieve column temperatures within the envelope 10–200 °C was of the order 25 W peak, two orders of magnitude less than conventional turbulent fans ovens. The performance of the device has been proven using a standard GC oven for injection, heating and FID detection. A low cost, low power photoionization detector has also been coupled to the glass column and the glass device heated directly via planar resistive elements. This low power GC-PID combination showed reasonable separation of a simple BTEX mixture in 230 s and with sub ng sensitivity.

The combination of a planar glass GC device with such a detector offers substantial potential as a field portable GC and is a useful alternative to typically square channelled silicon devices of restricted physical size and higher material cost. The larger glass wafer areas that may be micro-manufactured at reasonable costs (when compared to silicon) offers the potential for planar devices with column dimensions analogous to those used in laboratory GCs. In common with other planar GC approaches, the ability to directly cool this device using the Peltier effect may offer substantial advantages for the analysis of very volatile species over typical cryogenic cooling of drawn capillaries in standard GC ovens.

Acknowledgements

ACL and CNR received support from the Natural Environment Research Council under grant NE/F015240/1. JFH acknowledges support from the Yorkshire Enterprise Fellowship scheme, funded by Yorkshire Forward. JH acknowledges a PhD studentship supported by NPL. All NPL authors acknowledge funding from the Chemical and Biological Knowledge Base Programme of the National Measurement Office.

References

- [1] D. Helmig, W. Pollock, J. Greenberg, P. Zimmerman, J. Geophys. Res.: Atmos. 101 (1996) 14697.
- [2] B. Rappengluck, P. Fabian, Environ. Sci. Pollut. Res. 5 (1998) 65.
- [3] A.C. Lewis, N. Carslaw, P.J. Marriott, R.M. Kinghorn, P. Morrison, A.L. Lee, K.D. Bartle, M.J. Pilling, Nature 405 (2000) 778.
- [4] M. Ulman, K. Bielawska, B. Lozowicka, M. Heimann, J. Kesselmeier, G. Schebeske, K.S. Katrynski, Z. Chilmonczyk, Chem. Anal. 52 (2007) 435.
- [5] S.C. Terry, J.H. Jerman, J.B. Angell, IEEE Trans. Electron Devices 26 (1979) 1880.
- [6] Sandia National Laboratories, Microsensors and Sensor Microsystems - MicroChemLab, 2009. Available: <http://www.sandia.gov/mstc/MsensorSensorMsystems/MicroChemLab.html>, last accessed 30 July 2009.
- [7] D. Lindner, Lab Chip 1 (2001) 15N.
- [8] J.A. Potkay, G.R. Lambertus, R.D. Sacks, K.D. Wise, J. Microelectromech. Syst. 16 (2007) 1071.
- [9] S. Reidy, D. George, M. Agah, R. Sacks, Anal. Chem. 79 (2007) 2911.

- [10] R.R. Reston, E.S. Kolesar, J. Microelectromech. Syst. 3 (1994) 134.
- [11] G.R. Lambertus, C.S. Fix, S.M. Reidy, R.A. Miller, D. Wheeler, E. Nazarov, R. Sacks, Anal. Chem. 77 (2005) 7563.
- [12] J.B. Sanchez, F. Berger, M. Fromm, M.H. Nadal, Sens. Actuator B: Chem. 119 (2006) 227.
- [13] L. Lorenzelli, A. Benvenuto, A. Adami, V. Guarnieri, B. Margesin, V. Mulloni, D. Vincenzi, 8th World Congress on Biosensors, Elsevier Advanced Technology, Granada, Spain, 2004, p. 1968.
- [14] M. Nishino, Y. Takemori, S. Matsuoka, M. Kanai, T. Nishimoto, M. Ueda, K. Komori, IEEJ Trans. Electr. Electron. Eng. 4 (2009) 358.
- [15] A.D. Radadia, R.D. Morgan, R.I. Masel, M.A. Shannon, Anal. Chem. 81 (2009) 3471.
- [16] G. Lambertus, A. Elstro, K. Sensenig, J. Potkay, M. Agah, S. Scheuering, K. Wise, F. Dorman, R. Sacks, Anal. Chem. 76 (2004) 2629.
- [17] G. Lambertus, R. Sacks, Anal. Chem. 77 (2005) 2078.
- [18] E.T. Zellers, S. Reidy, R.A. Veeneman, R. Gordenker, W.H. Steinecker, G.R. Lambertus, K. Hanseup, J.A. Potkay, M.P. Rowe, Z. Qiongyan, C. Avery, H.K.L. Chan, R.D. Sacks, K. Najafi, K.D. Wise, Solid-State Sensors, Actuators and Microsystems Conference, 2007. TRANSDUCERS 2007. International, 2007, p. 1491.
- [19] S.E. Lewis, J.R. DeBoer, J.L. Gole, P.J. Hesketh, Sens. Actuator B: Chem. 110 (2005) 54.
- [20] M. Stadermann, A.D. McBrady, B. Dick, V.R. Reid, A. Noy, R.E. Synovec, O. Bakajin, Anal. Chem. 78 (2006) 5639.
- [21] H.S. Noh, P.J. Hesketh, G.C. Frye-Mason, J. Microelectromech. Syst. 11 (2002) 718.
- [22] A. Bhushan, D. Yemane, E.B. Overton, J. Goettert, M.C. Murphy, J. Microelectromech. Syst. 16 (2007) 383.
- [23] B. Dziurdzia, Z. Magonski, S. Nowak, Meas. Sci. Technol. 19 (2008) 6.
- [24] A. Bhushan, D. Yemane, D. Trudell, E.B. Overton, J. Goettert, 6th Biennial International Workshop on High Aspect Ratio Micro Structure Technology, Springer, Gyenogju, South Korea, 2005, p. 361.
- [25] S.R. Sumpter, M.L. Lee, J. Microcolumn Sep. 3 (1991) 91.
- [26] R.S. Pai, D.R. Mott, J.L. Stepnowski, R.A. McGill, B.A. Higgins, D.L. Simonson, IEEE Conference on Technologies for Homeland Security, IEEE, Waltham, MA, 2008, p. 150.
- [27] Agilent Technologies, 3000 Micro GC, 2009. Available: <http://www.chem.agilent.com/en-US/Products/Instruments/gc/3000microgc/Pages/default.aspx>, last accessed 30 July 2009.
- [28] C2V, C2V-200 micro GC, 2009. Available: http://www.c2v.nl/products/instrumentation/C2V_200_micro_gc.shtml, last accessed 30 July 2009.
- [29] SLS Micro Technology, GCM 5000, 2003. Available: <http://www.sls-micro-technology.de/146.html>, last accessed 30 July 2009.
- [30] E.J. Staples, S. Viswanathan, Ind. Eng. Chem. Res. 47 (2008) 8361.
- [31] A. Modi, N. Koratkar, E. Lass, B. Wei, P.M. Ajayan, Nature 424 (2003) 171.
- [32] T.C. Hayward, K.B. Thurbide, 31st International Symposium on Capillary Chromatography, Elsevier Science Bv, Albuquerque, NM, 2007, p. 2.
- [33] T.C. Hayward, K.B. Thurbide, Talanta 73 (2007) 583.
- [34] K.B. Thurbide, T.C. Hayward, Anal. Chim. Acta 519 (2004) 121.